# Experimental Status on the Proton Charge Radius

**Haiyan Gao**[*a], **Vladimir Khachatryan**[a], **and Jingyi Zhou**[a]

[a]*Department of Physics, Duke University, Durham, NC 27708, USA*

*E-mail:* haiyan.gao@duke.edu, vladimir.khachatryan@duke.edu, jingyi.zhou@duke.edu

In this proceedings, we present the experimental status of measurements of the charge radius of the proton. Its accurate knowledge is not only important for understanding how Quantum Chromodynamics (QCD) is manifested in the non-perturbative QCD region, but also is essential for carrying out bound state Quantum Electrodynamics (QED) calculations of atomic energy levels. We discuss the methods and types of measurements performed during the last dozen of years, for determining that radius. We also discuss the current status of the proton charge radius puzzle, as well as give some details on various upcoming experiments. In the light of such new experimental results, the ultimate resolution of the radius puzzle may be addressed in the foreseeable future.

*CD2021: The 10th International Workshop on Chiral Dynamics*
*November 15 - 19, 2021*
*Beijing, China*

---

[*]Speaker.

## 1. Introduction

While QCD in the perturbative region has been well tested by experiments at high energies, understanding QCD in the non-perturbative region remains a challenge. In this context, the nucleons are remarkable fermi-sized laboratories to gain important knowledge on how non-perturbative QCD works in the low-energy region. In particular, there have been and are ongoing enormous experimental and theoretical efforts invested for understanding the internal structure and properties of the proton, such as its spin [1, 2, 3] and mass [4, 5, 6, 7, 8].

In this proceedings paper we will be focusing on the experimental status of the proton's root-mean-square (rms) charge radius, $r_{p,rms} \equiv r_p$ [9] – a conventional measure for the proton's size – which is directly related to the slope of the electric form factor, $G_E^p$, at $Q^2 = 0$ (with $Q^2$ being the four-momentum transfer squared)

$$r_p \equiv r_{E,rms}^p = \sqrt{\langle r_E^2 \rangle} = \left[ -\frac{6}{G_E^p(0)} \frac{dG_E^p(Q^2)}{dQ^2} \Big|_{Q^2=0} \right]^{1/2}, \tag{1.1}$$

where $G_E^p(0) = 1$. The charge radius of the proton is a quantity, which is important both for QCD as well as for bound state QED calculations of atomic energy levels that is critical in determining the Rydberg constant [10], one of the most well-known fundamental quantities in nature.

In 2010, the so-called proton charge radius puzzle appeared, which at that time indicated a significant discrepancy of $\sim 7$ standard deviation between the radius value measured by the high precision muonic hydrogen spectroscopy [11] and the world-average $r_p$ value determined by the 2010 Committee on Data for Science and Technology (CODATA) based on measurements of the ordinary (atomic) hydrogen spectroscopy and electron-proton scattering experiments [12]. This puzzle afterwards triggered more intensive experimental/theoretical efforts to re-measure/re-calculate the $r_p$ value.

## 2. Electron-proton elastic scattering

In this section we briefly describe three electron-proton elastic scattering experiments, however, we wish to start with introducing pertinent experimental techniques for measuring the proton electromagnetic form-factors and their ratios. Those form factors describe the spatial distribution of charge and magnetization within the proton [13, 14, 15].

(1) *Unpolarized elastic $e-p$ cross section with the Rosenbluth separation.*

Using the one-photon exchange approximation, one can write the differential cross section of unpolarized elastic $e-p$ scattering via the Rosenbluth formula [16, 17]:

$$\frac{d\sigma}{d\Omega} = \frac{\alpha^2 \cos^2(\theta/2)}{4E^2 \sin^4(\theta/2)} \frac{E'}{E} \left[ \frac{(G_E^p)^2 + \tau(G_M^p)^2}{1+\tau} + 2\tau(G_M^p)^2 \tan^2(\theta/2) \right], \tag{2.1}$$

where $\tau = Q^2/(4M_p^2)$, $M_p$ proton mass and $\theta$ electron scattering angle. In the Rosenbluth separation method, the proton electric $(G_E^p)^2$ and magnetic $(G_M^p)^2$ form factor squared are separated by measuring the cross section with changing beam energies $E$ and electron scattering angles $\theta$ but with fixed $Q^2$. But it is difficult to extract $G_E^p$ at high $Q^2$ and $G_M^p$ at low $Q^2$ precisely using this

method because in Eq. (2.1) the contribution from $G_E^p$ term becomes dominant as $Q^2$ decreases, while $G_M^p$ term dominates the cross section in the high $Q^2$ region.

(2) *Recoil proton polarization measurement with a polarized beam only*:

Experimental methods that use polarization degrees of freedom in electron scattering experiments provide an access to the form factor interference term, $G_E^p G_M^p$, which does not suffer from the $Q^2$-dependent sensitivity as does the Rosenbluth method when extracting $G_E^p$ at high and extracting $G_M^p$ at low $Q^2$. In experiments based on the elastic scattering of longitudinally polarized electrons from unpolarized protons, one can extract the form-factor ratio $G_E^p/G_M^p$ by simultaneously measuring the transverse ($P_l$) and longitudinal ($P_t$) polarizations of the recoil proton:

$$\frac{G_E^p}{G_M^p} = -\frac{P_t}{P_l} \frac{E + E^{'}}{2M_p} \tan(\theta/2). \tag{2.2}$$

The recoil proton polarizations are determined from azimuthal distributions obtained after the recoil protons scatter off specific analyzer material (like carbon). Some factors that would introduce experimental uncertainties are canceled by using this technique, such as the detector efficiency, luminosity, and the analyzing power of proton polarimeter. If we combine the cross-section and recoil proton polarization measurements, then one can determine both form factors precisely, regardless of their $Q^2$ sensitivity.

(3) *Asymmetry (super-ratio) measurement with polarized beam and polarized target*:

There is another method to extract the ratio $G_E^p/G_M^p$ by measuring the asymmetry from the elastic scattering of longitudinally polarized electrons from polarized protons, which is expressed as

$$A_{\text{exp}} = P_b P_t \frac{-2\tau \nu_{T'} \cos\theta^* (G_M^p)^2 + 2\sqrt{2\tau(1+\tau)}\, \nu_{TL'} \sin\theta^* \cos\varphi^* G_M^p G_E^p}{(1+\tau)\nu_L (G_E^p)^2 + 2\tau \nu_T (G_M^p)^2}, \tag{2.3}$$

where $P_b$ and $P_t$ are the beam and target polarizations, $\theta^*$ and $\varphi^*$ are the polar and azimuthal angles of the proton polarization with respect to the virtual photon's three-momentum transfer and the scattering plane. Besides, the kinematic factors $\nu_{T'}$, $\nu_{TL'}$, $\nu_T$, and $\nu_L$ can be found in [18]. Then the ratio $G_E^p/G_M^p$ can be determined by taking a "super ratio", if one uses a symmetric detector configuration [19]:

$$R_A = \frac{A_{\text{exp},1}}{A_{\text{exp},2}} = \frac{a_1 - b_1 \ G_E^p/G_M^p}{a_2 - b_2 \ G_E^p/G_M^p}, \tag{2.4}$$

where $A_{\text{exp},1}$ and $A_{\text{exp},2}$ will be the measured asymmetries in the two symmetric detectors, the proton polarization is fixed in the laboratory frame. This technique also benefits from the cancellation of detector efficiency, beam/target polarizations, and luminosity factors.

## 2.1 The Mainz A1 experiment

An unpolarized $e - p$ elastic scattering experiment has been performed by the A1 collaboration at Mainz Microtron (MAMI) [20, 21]. Electron beams at six different energies (180, 315, 450, 585, 720, and 855 MeV) were used in this experiment. Three rotatable high-resolution magnetic spectrometers were used to monitor the luminosity and measure the scattered electrons at various scattering angles. In total, 34 sets of the 1422 differential cross-section data points with statistical error $\leq 0.2\%$ were measured covering a $Q^2$ range of $0.0038 - 0.9772$ (GeV/c)$^2$.

Bernauer *et al.* have carried out comprehensive studies of model dependence in the proton form factors' extraction, then obtained $r_p$ using fits of the spline and polynomial function groups. The extracted result is $r_p = 0.879(5)_{stat}(4)_{sys}(2)_{mod}(4)_{group}$ fm, which is consistent with the CODATA-2006 world-average value [22] but ~ $5.7\sigma$ higher than the muonic hydrogen results[11, 23].

## 2.2 The JLab recoil polarization experiment

The recoil proton polarization experiment conducted in Hall A at Jefferson Lab has utilized a recoil proton polarimeter to measure the polarization transfer in the $e - p$ elastic scattering [24]. This experiment has used a 1.192 GeV longitudinally polarized electron beam and a 6-cm long unpolarized liquid Hydrogen target. A large acceptance spectrometer "BigBite" was used to measure the scattered electrons, and a high resolution spectrometer (HRS) was used to detect the recoil protons, and a focal plane polarimeter was used to measure the recoil proton polarization. The proton form-factor ratio $\propto_p G_E^p/G_M^p$ was extracted with a total uncertainty of ~ 1% in a $Q^2$ range of $0.3 - 0.7$ (GeV/c)$^2$. After combining these results with the other proton form-factor ratio measurements at JLab [25, 26, 27], a global fitting was performed resulting in $r_p = 0.875 \pm 0.010$ fm. Without including the Mainz data in the global fit, this radius value is in good agreement with the results from the Mainz experiment mentioned in Sec. 2.1 and from the CODATA-2006 [22] $r_p$ value.

## 2.3 The JLab PRad experiment

The proton charge radius experiment (PRad) in Hall B at Jefferson Lab [28] has used a magnetic-spectrometer-free calorimeter based method, which was unique compared to the other elastic $e - p$ scattering experiments carried out previously. This method allowed the experiment to measure the scattered electrons in scattering angles as forward as ~ 0.7° and in a large angular range within one fixed setting, without moving any of the detectors that would introduce normalization uncertainties among different angles. The PRad experiment was operating with electron beams at 1.1 and 2.143 GeV, and measuring the $e - p$ elastic scattering cross section in an unprecedentedly low $Q^2$ range ($2 \times 10^{-4} - 5 \times 10^{-2}$ (GeV/c)$^2$), which is essential for extracting $r_p$ precisely from the slope of $G_E^p$ in the limit of $Q^2 = 0$ (see Eq. (1.1)).

The PRad experimental setup is shown in Fig. 1. A windowless gas flow hydrogen target was used to suppress the background and details of this target can be found in [29]. Next to the target, a 5-meter long two-stage vacuum chamber was used to further remove backgrounds from multiple scatterings of the scattered electrons. A large plane of Gas Electron Multiplier (GEM) detectors was used for electron tracking. Also, a hybrid electromagnetic calorimeter (HyCal) with high resolution and efficiency was used for energy and scattering angle measurement. To control the systematic uncertainties, the well-known QED Møller process ($e^- e^- \rightarrow e^- e^-$) was measured simultaneously during the experiment and used for normalization.

In addition, the PRad collaboration carried out a robust fitter (a functional form for the $r_p$ extraction) study in [30] and found that the Rational (1,1) function is the best fitter for determining the radius and for controlling the fitting uncertainty:

$$f(Q^2) = nG_E(Q^2) = n\frac{1 + p_1Q^2}{1 + p_2Q^2}. \tag{2.5}$$

First, the proton electric form factor was extracted from the measured cross-section data, and then the radius was obtained using the Rational (1,1) functional fit [31].     The extracted charge radius value is $r_p = 0.831 \pm 0.007(\text{stat}) \pm 0.012(\text{syst})$ fm, which is in agreement with the muonic hydrogen spectroscopic results [11, 23], and the recent measurement from ordinary hydrogen Lamb shift [32].
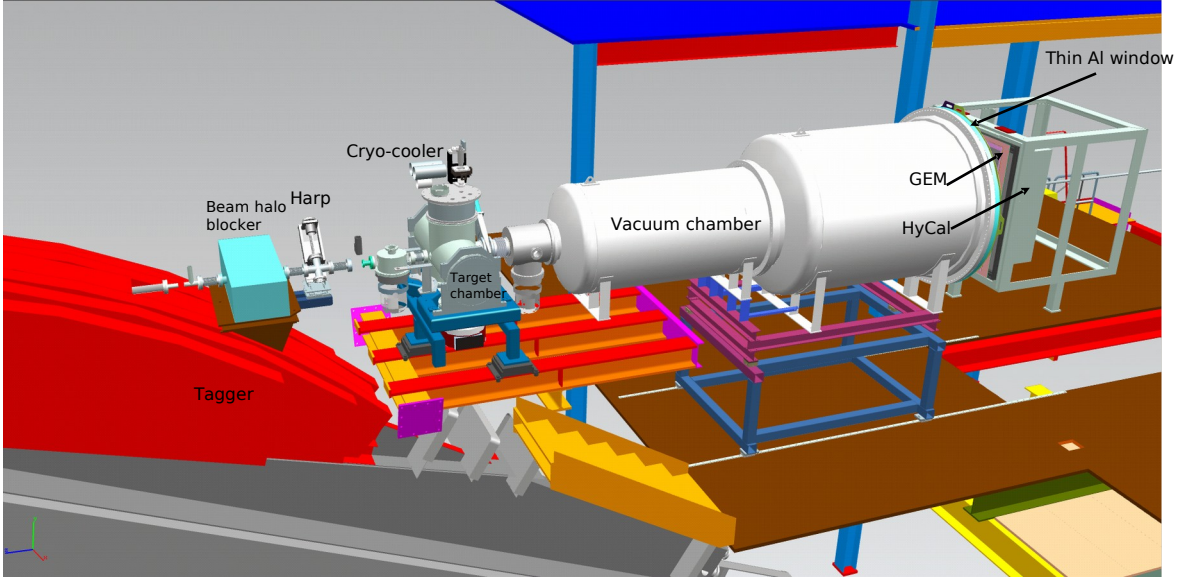


**Figure 1:** The layout of the PRad experiment in Hall B at Jefferson Lab.     The incident electron beam is designed to be from left to right. The figure is from [33].
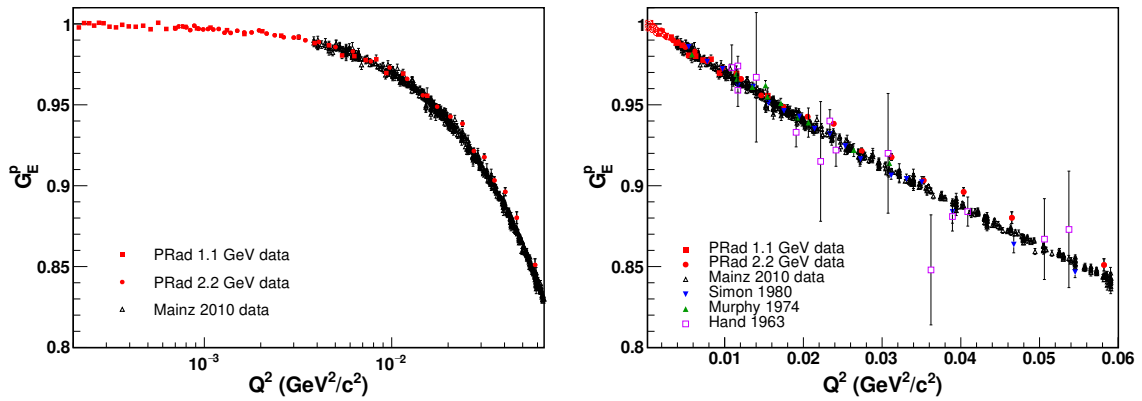


**Figure 2:** (Left panel) The proton electric form factor $G_E^p(Q^2)$ data obtained from the PRad measurement [28] and from the Mainz measurement [20] in the overlap $Q^2$ region of the data from both experiments. (Right panel) The data in the left panel plot plus also form-factor data from [34], [35], [36], all shown on linear scale. The figure is from [9] and [31].

## 3. Atomic and muonic hydrogen spectroscopy

### 3.1 Atomic H spectroscopy measurements

QED calculations of atomic spectroscopy include the corrections for the finite size of the

proton. By comparing the measurements with state-of-the-art calculations, one can a produce a very precise value of the proton rms charge radius. In the recent few years, four modern atomic hydrogen spectroscopy measurements have been performed with major improvements compared to similar previous measurements [32, 37, 38, 39]. Bezginov *et al.* [32] performed a measurement of the hydrogen Lamb shift in $2S_{1/2}$-$2P_{1/2}$ transition, and extracted $r_p$ directly by comparing with QED calculations. Beyer *et al.* [37] measured the 2S-4P transition of ordinary hydrogen atom (showed in Fig. 3) along with a few improvements. Fleurbaey *et al.* [38] and Grinin *et al.* [39] measured the 1S-3S transition of ordinary hydrogen atoms. These latter three experiments combined their results with the previous 1S-2S transition frequency measurements to obtain $r_p$. And Fig. 5 shows the measured proton radii from the four atomic H spectroscopy measurements discussed here.
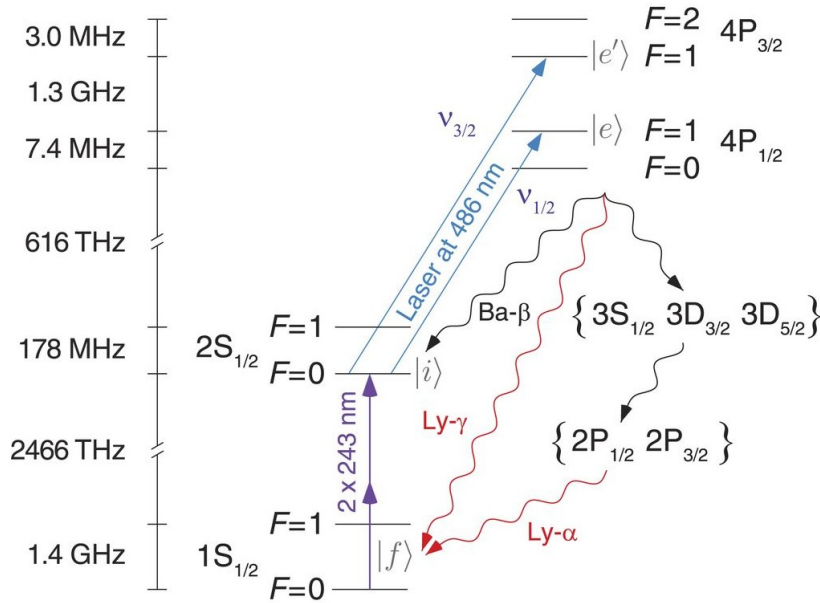


**Figure 3:** The energy levels of atomic hydrogen relevant to the $r_p$ measurement. The figure is from [37].

## 3.2 Muonic H spectroscopy measurements

In muonic hydrogen, the orbital electron is replaced by the muon. The muon is ~200 times heavier than the electron, so that it orbits much closer to the proton and is more sensitive to the proton finite size effect. The first muonic hydrogen spectroscopy measurement was conducted at the Paul Scherrer Institute (PSI) [11]. Pohl *et al.* measured the transition frequency of the muonic hydrogen between the $2S_{1/2}^{F=1}$ and the $2P_{3/2}^{F=2}$ states. Antognini *et al.* [23] mearsured not only the transition between $2S_{1/2}^{F=1}$ and $2P_{3/2}^{F=2}$ states but also the transition between $2S_{1/2}^{F=0}$ and $2P_{3/2}^{F=1}$ states, as shown in Fig. 4. The results from these two high-precision measurements are consistent with each other.

## 4. Proton charge radius puzzle

Fig. 5 shows the results from the atomic H and muonic H spectroscopy measurements discussed in Sec. 3. The result from the atomic H spectroscopy by Fleurbaey *et al.* [38] is consistent
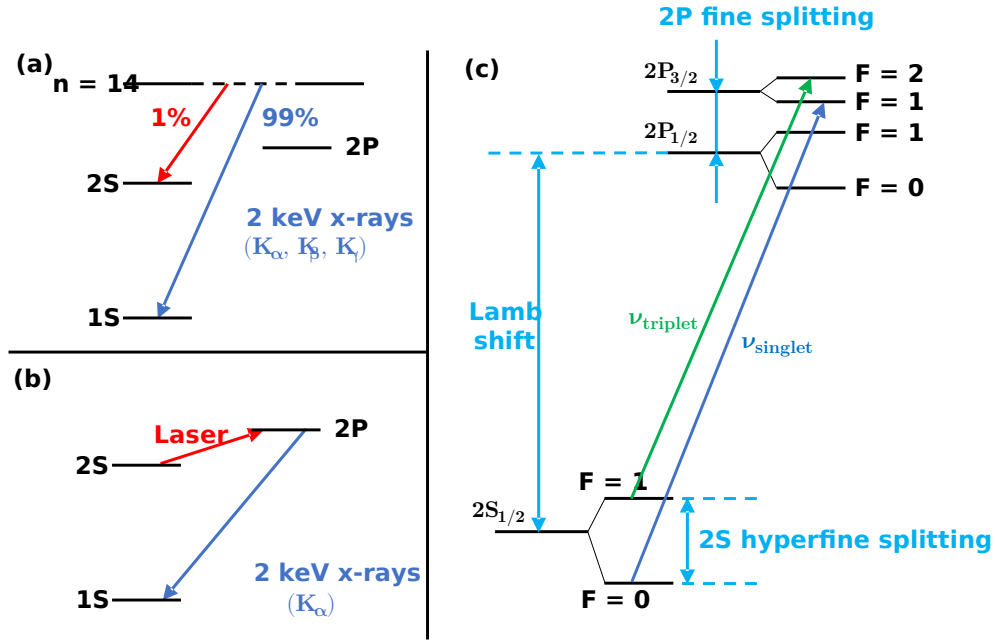
**Figure 4:** The energy levels of muonic hydrogen relevant to the $r_p$ measurement. The figure is from [9].

with the CODATA-2014 recommended value [40]. However, the $r_p$ values from the other three atomic measurements [32, 37, 39] are smaller than the CODATA-2014 recommended value by 3-4 standard deviation and are consistent with the two results from the muonic spectroscopy measurements [11, 41], as well as consistent with the result from the PRad $e − p$ elastic scattering experiment [28]. The proton radius extracted from the $e − p$ elastic scattering experiments discussed in Sec. 2 and from various analyses including global fits carried out in recent years are summarized in Fig. 6. The CODATA-2014 recommended value and the two results from the muonic spectroscopy experiments are also included for comparison.

Discrepancies exist between the same type of experiments, such as the $e − p$ elastic scattering results from Mainz [21] and PRad [28], and between the results from the four atomic spectroscopy measurements. Moreover, re-analyses of the same experimental data using different methods also yield different $r_p$ values. For example, [42, 43, 44, 45, 46, 47] analyzed the same sets of Mainz data, and the results from Lorenz *et al.* [42], Griffioen *et al.* [44], Alarcon *et al.* [46], Cui *et al.* [47] are consistent with the muonic H measurements within their quoted uncertainties, however, Lee *et al.* [43] supports the Mainz original result [21].

Until now, no widely accepted conclusion exists to address the proton charge radius puzzle very satisfactorily. As a result, future higher precision measurements in atomic H spectroscopy and lepton scattering experiments are still essential.
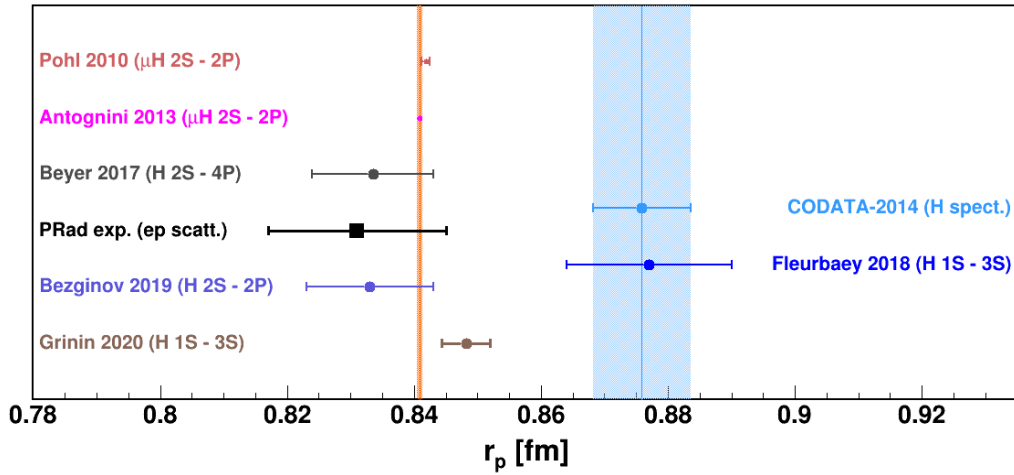
**Figure 5:** The latest $r_p$ results from atomic spectroscopy measurements together with muonic spectroscopy results, as well as the CODATA-2014 recommended value based on ordinary atomic spectroscopy and the most recent result from electron scattering.
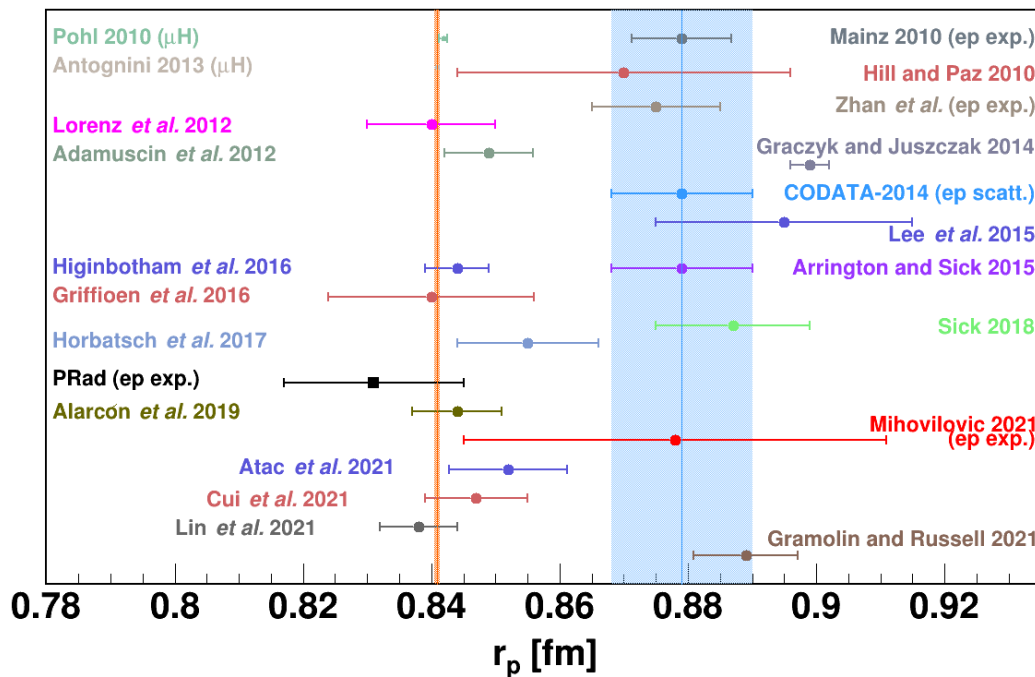


**Figure 6:** The $r_p$ values determined from electron scattering experiments (performed after 2010) together with the results from various (re-)analyses of $e - p$ scattering data.

## 5. Upcoming lepton-proton experiments for the $r_p$ measurements

### 5.1 The JLab PRad-II (upgraded PRad) experiment

The PRad experiment has shown the advantage of its new and unique experimental setup for successfully carrying out an $e - p$ elastic scattering experiment but has not reached yet its ultimate

precision in determination of $r_p$. Based on the PRad experiment, the upgraded PRad-II experiment was proposed [48] and approved by JLab PAC in 2020, which will reach an even lower $Q^2$ region ($\sim 10^{-5}$ (GeV/C)$^2$).

As shown in Fig. 7, two planes of tracking detectors made by new technology ($\propto$RWell) with excellent position resolution will be utilized for tracking the scattered electrons. Compared to the PRad experiment that has only one plane of GEM-based detectors, the two new tracking detectors will further suppress the beamline background from the upstream collimator. This major upgrade will also allow the experiment to achieve much higher precision in the angle reconstruction of the scattered electrons as well as in the $Q^2$ determination, especially at very small scattering angles ($< 1^\circ$). An upgraded calorimeter built entirely from PbWO$_4$ modules with high resolution and efficiency will improve the energy resolution and help further veto the inelastic background of the experiment. In order to reach the lowest possible $Q^2$ by measuring the scattered electrons down to $0.5^\circ$, a cross-shaped scintillator detector will be placed inside the target chamber. The purpose of this detector is to improve the separation between the elastic $e-p$ events and the Møller events in the scattering angular range between $0.5^\circ - 0.8^\circ$. Last but not least, new higher-order radiative correction calculations will help control the uncertainty in the Born cross section extraction from the experimental data.
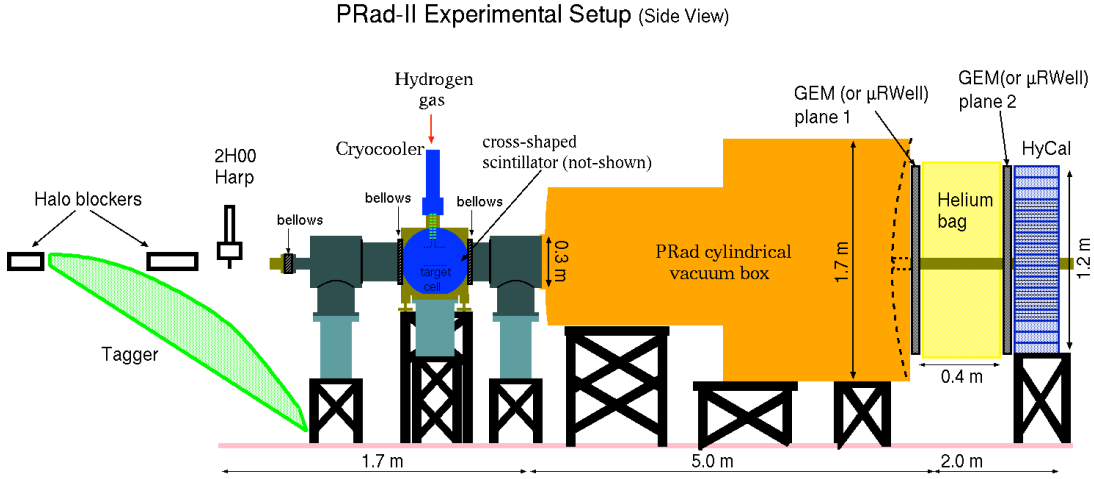


**Figure 7:** The layout of the proposed PRad-II experiment in Hall B at Jefferson Lab. The incident electron beam is designed to be from left to right. This figure is from [9].

With the aforementioned improvements, the overall experimental uncertainties are determined to be reduced by a factor of 3.8 compared to those of PRad. The proton radius projection of the PRad-II experiment is shown in Fig. 8. In this figure, the blue line and its band represent the weighted average and the total uncertainty of the $r_p$ results from PRad [28] and the two ordinary hydrogen spectroscopic measurements [37, 32]. The grey line and its band are the weighted average and the total uncertainty of the three results in the blue band as well as the $r_p$ value from [39]. These two bands indicate the importance of performing higher precision measurements on electron systems, including both the $e-p$ scattering and ordinary hydrogen spectroscopy measurements. Besides, the upcoming PRad-II experiment will be important to address an issue on whether there is a discrepancy in results from the electronic versus muonic systems (the lepton universality).
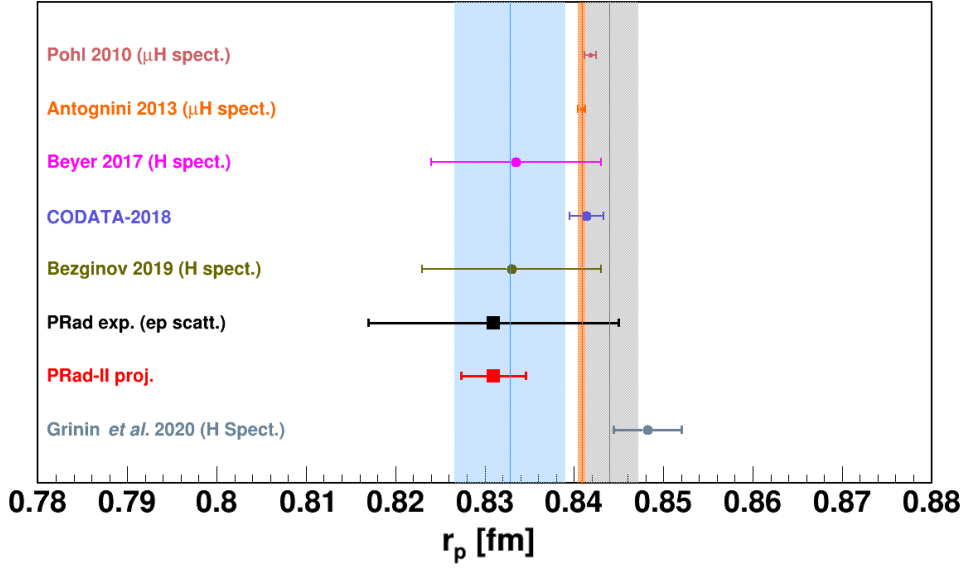
**Figure 8:** The projection for $r_p$ based on all PRad-II proposed upgrades and improvements, shown with a few chosen radius results from other experiments and CODATA-2018 recommendation.

## 5.2 Other experiments

In addition to the PRad-II experiment, there are also other ongoing and upcoming lepton-proton elastic scattering experiments at different facilities. A summary of their $Q^2$ kinematic ranges and the projected precision is given in Table. 1, as well as a brief introduction about each experiment is discussed in the following.

| Experiment | Beam | Laboratory | $Q^2$ (GeV/c)$^2$ | $\delta r_p$ ($fm$) | Status |
|---|---|---|---|---|---|
| PRad-II | $e^-$ | Jefferson Lab | $4 \times 10^{-5} - 6 \times 10^{-2}$ | 0.0036 | Future |
| MUSE | $e^\pm, \propto^\pm$ | PSI | $0.0015 - 0.08$ | 0.01 | Ongoing |
| AMBER | $\propto^\pm$ | CERN | $0.001 - 0.04$ | 0.01 | Future |
| A1@MAMI | $e^-$ | Mainz | $0.004 - 0.085$ | | Ongoing |
| MAGIX@MESA | $e^-$ | Mainz | $\geq 10^{-4} - 0.085$ | | Future |
| PRES | $e^-$ | Mainz | $0.001 - 0.04$ | 0.6% (rel.) | Future |
| ULQ$^2$ | $e^-$ | Tohoku Uni. | $3 \times 10^{-4} - 8 \times 10^{-3}$ | ~1% (rel.) | Future |

**Table 1:** The ongoing and upcoming experiments for measuring $r_p$ and their current status [9, 49, 50, 51, 52, 53, 54, 55].

*The MUSE Experiment at PSI* [49]: The MUon Scattering Experiment (MUSE) at PSI is a scattering experiment that is ongoing aiming to resolve the $r_p$ puzzle. It measures the charge radius of the proton from the $\propto^\pm - p$ and $e^\pm - p$ elastic scattering cross sections based upon an experimental setup shown in Fig. 9. In addition to extracting $r_p$, the two-photon-exchange effect (TPE) in the lepton scattering can be tested by comparing the $\propto^\pm - p$ and $e^\pm - p$ elastic scattering cross sections.
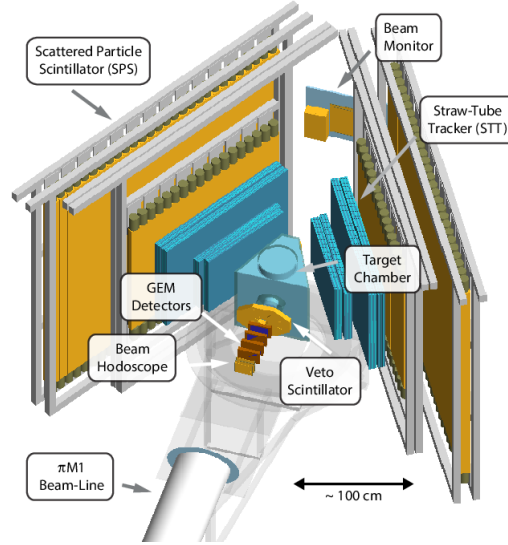
**Figure 9:** The schematic view of the MUSE experimental setup. This figure is from [50].

*The AMBER Experiment at CERN* [51]:   Fig. 10 shows a layout of the experimental setup required for the $r_p$ measurement in high-energy low-$Q^2$ elastic $\propto - p$ scattering at the M2 beam line of the CERN Super Proton Synchrotron (SPS). The muon beam energy in the experiment is at 100 GeV, which in certain circumstances has advantages for systematics compared to the low energy lepton-proton scattering experiments. This experiment will not only measure the scattered muons with the AMBER spectrometer but also measure the recoil protons with a hydrogen time-projection chamber (TPC).
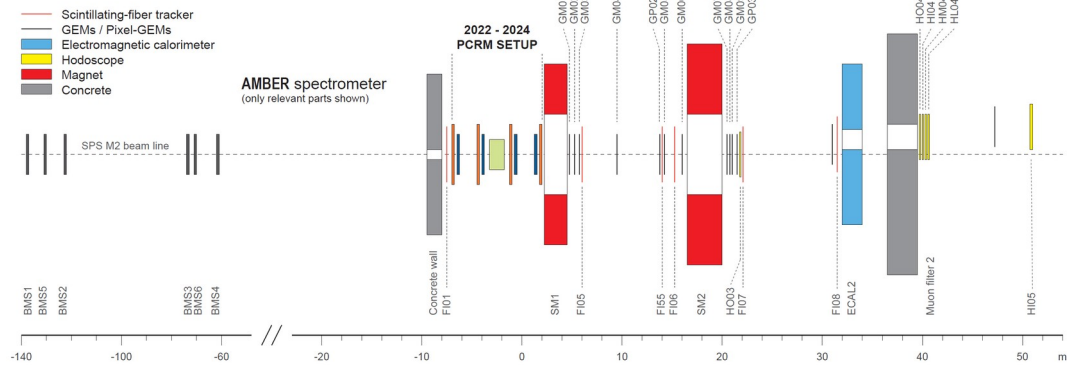


**Figure 10:** The schematic view of the experimental setup at the M2 beam line,    highlighting the relevant parts of the AMBER spectrometer and the additional detectors required for the $r_p$ measurement. This figure is from [51].

There are two new programs at Mainz University for measuring the elastic electron scattering, with a goal to add new inputs in further resolution of the proton charge radius puzzle.

*The A1@MAMI and MAGIX@MESA Experiments at Mainz* [52, 53]:   The A1@MAMI experiment is an ongoing experiment conducted in the A1 experimental hall at MAMI. This experiment

is an upgrade of the original A1 experiment [20] that utilizes a hydrogen gas-jet target to better control certain systematic uncertainties.

The MAinz Gas Injection target eXperiment (MAGIX) will employ a multi-purpose spectrometer system in the Energy Recovery Linac (ERL) arc of the new Mainz Energy Recovering Superconducting Accelerator (MESA), along with using a gas jet target at its center. The proton radius will be determined from the electron scattering data measured from the elastic electron scattering at low $Q^2$, reaching down to below $10^{-4}$ $(\text{GeV/c})^2$. A relatively clean environment and high luminosity can be achieved in this experiment due to the ultra-light gas target and high-intensity electron beam.
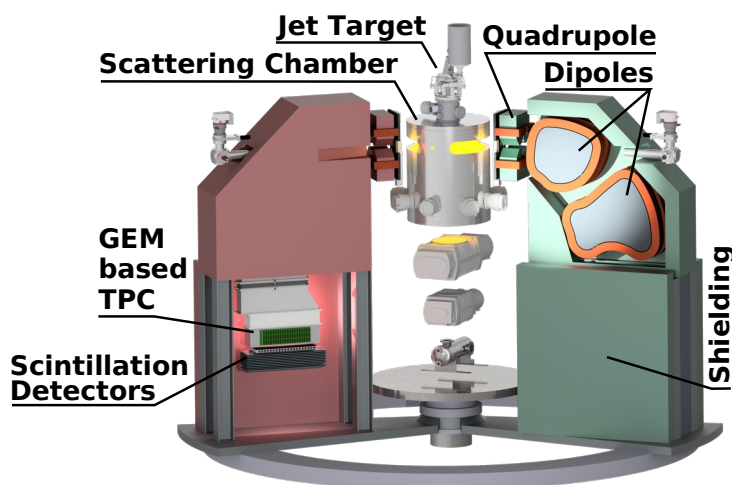


**Figure 11:** The layout of the planned MAGIX spectrometer setup at the MESA. This figure is from [53].

*The PRES Experiment at Mainz* [54]: The PRES experiment will be performed in the A2 experimental Hall at MAMI. Similar to the AMBER experiment, both the scattered electrons and recoil protons will be measured. Taking the advantage of a similar setup, the results from the two experiments can be combined to investigate the lepton universality.

*The Ultra-Low $Q^2$ (ULQ$^2$) experiment at Tohoku University* [55]: This experiment will use 20-60 MeV electron beams to measure scattered electrons in the angular range from $30^\circ$ to $150^\circ$, which will allow the experiment to reach low $Q^2$ of $3 \times 10^{-4}$ $(\text{GeV/c})^2$. Simultaneously, the elastic $e - {}^{12}C$ process will be measured for normalization.

## 6. Summary

In this proceedings, we outlined experimental techniques and various experiments conducted in recent years for measuring the proton rms charge radius. We also discussed the current status of the proton charge radius puzzle and future related experiments. After years of experimental efforts, major progress has been made, but the puzzle is not fully resolved yet. The smaller radius values reported by PRad [28] and two recent ordinary atomic H spectroscopy measurements [37, 32], within their experimental uncertainties, are in agreement with the muonic H spectroscopy measurement outcomes [11, 41]. Nonetheless, the most recent and most precise atomic spectroscopy

measurement [39] extracted a radius value, which is larger than the muonic results for about two standard deviations (see Fig. 5 or Fig. 8). What made the puzzle even more attractive and challenging is a possible lepton universality problem that arises from the discrepancy between $r_p$ obtained from the electronic and muonic systems. New experiments with higher precision and with different types of lepton beams (by having various energies) may shed light on answering these long-awaited fundamental questions.

## 7. Acknowledgements

## References

[1] X. Ji, F. Yuan and Y. Zhao, *What we know and what we don't know about the proton spin after 30 years*, *Nature Rev. Phys.* **3** (2021) 27 [2009.01291].

[2] S.E. Kuhn, J.P. Chen and E. Leader, *Spin Structure of the Nucleon - Status and Recent Results*, *Prog. Part. Nucl. Phys.* **63** (2009) 1 [0812.3535].

[3] J. Ashman et al., *A measurement of the spin asymmetry and determination of the structure function $g_1$ in deep inelastic muon-proton scattering*, *Physics Letters B* **206** (1988) 364.

[4] X. Ji, *QCD Analysis of the Mass Structure of the Nucleon*, *Phys. Rev. Lett.* **74** (1995) 1071.

[5] C. Lorcé, *On the hadron mass decomposition*, *The European Physical Journal C* **78** (2018) 120.

[6] H. Gao et al., *Proton remains puzzling*, *The Universe* **3** (2015) 18.

[7] O. Gryniuk and M. Vanderhaeghen, *Accessing the real part of the forward $J/\psi$-p scattering amplitude from $J/\psi$ photoproduction on protons around threshold*, *Phys. Rev. D* **94** (2016) 074001.

[8] Jefferson Lab Proposal E12-12-006, Spokespersons: K. Hafidi, X. Qian, N. Sparveris, Z.-E. Meziani (contact), and Z. W. Zhao, *Near Threshold Electroproduction of $J/\Psi$ at 11 GeV*, 2012.

[9] H. Gao and M. Vanderhaeghen, *The proton charge radius*, *Rev. Mod. Phys.* **94** (2022) 015002 [2105.00571].

[10] E. Tiesinga, P.J. Mohr, D.B. Newell and B.N. Taylor, *CODATA recommended values of the fundamental physical constants: 2018\**, *Rev. Mod. Phys.* **93** (2021) 025010.

[11] R. Pohl et al., *The size of the proton*, *Nature* **466** (2010) 213.

[12] P.J. Mohr, B. Taylor and D. Newell, *CODATA recommended values of the fundamental physical constants: 2010\**, *Rev. Modern Physics* **84** (2012) 1527.

[13] J. Arrington, C.D. Roberts and J.M. Zanotti, *Nucleon electromagnetic form-factors*, *J. Phys. G* **34** (2007) S23 [nucl-th/0611050].

[14] C.F. Perdrisat, V. Punjabi and M. Vanderhaeghen, *Nucleon Electromagnetic Form Factors*, *Prog. Part. Nucl. Phys.* **59** (2007) 694.

[15] V. Punjabi, C.F. Perdrisat, M.K. Jones, E.J. Brash and C.E. Carlson, *The Structure of the Nucleon: Elastic Electromagnetic Form Factors*, *Eur. Phys. J. A* **51** (2015) 79 [1503.01452].

[16] M. Rosenbluth, *High Energy Elastic Scattering of Electrons on Protons*, *Phys. Rev.* **79** (1950) 615.

[17] I.A. Qattan et al., *Precision Rosenbluth Measurement of the Proton Elastic Form Factors*, *Phys. Rev. Lett.* **94** (2005) 142301.

[18] T.W. Donnelly and A.S. Raskin, *Considerations of polarization in inclusive electron scattering from nuclei*, *Annuals of Physics* **169** (1986) 247.

[19] C. Crawford et al., *Measurement of the Proton's Electric to Magnetic Form Factor Ratio from $^1\vec{H}(e,e^{'})$*, *Phys. Rev. Lett.* **98** (2007) 052301.

[20] J. Bernauer et al., *High-Precision Determination of the Electric and Magnetic Form Factors of the Proton*, *Phys. Rev. Lett.* **105** (2010) 242001.

[21] A1 collaboration, *Electric and magnetic form factors of the proton*, *Phys. Rev. C* **90** (2014) 015206.

[22] P.J. Mohr, B. Taylor and D. Newell, *CODATA recommended values of the fundamental physical constants: 2006\**, *Rev. Modern Physics* **80** (2008) 633.

[23] A. Antognini et al., *Proton Structure from the Measurement of 2S-2P Transition Frequencies of Muonic Hydrogen*, *Science* **339** (2013) 417.

[24] X. Zhan et al., *High-precision measurement of the proton elastic form factor ratio $\frac{G_E}{G_M}$ at low $Q^2$*, *Physics Letters B* **705** (2011) 59.

[25] E03-104 C OLLABORATION collaboration, *Polarization Transfer in the $^4$He$(\vec{e},e^{'}\,\vec{p})^3$H Reaction at $Q^2 = 0.8$ and 1.3 $(GeV/c)^2$*, *Phys. Rev. Lett.* **105** (2010) 072001.

[26] A.J.R. Puckett et al., *Recoil Polarization Measurements of the Proton Electromagnetic Form Factor Ratio to $Q^2 = 8.5\,GeV^2$*, *Phys. Rev. Lett.* **104** (2010) 242301.

[27] G. Ron et al., *Low-$Q^2$ measurements of the proton form factor ratio $\propto_p GE/GM$*, *Phys. Rev. C.* **84** (2011) 055204.

[28] W. Xiong et al., *A small proton charge radius from an electron–proton scattering experiment*, *Nature* **575** (2019) 147.

[29] J. Pierce et al., *The PRad Windowless Gas Flow Target*, 2021.

[30] X. Yan et al., *Robust extraction of the proton charge radius from electron-proton scattering data*, *Phys. Rev. C* **98** (2018) 025204.

[31] W. Xiong, *A High Precision Measurement of the Proton Charge Radius at JLab*, Ph.D. thesis, Duke University, 2020.

[32] N. Bezginov, T. Valdez, M. Horbatsch, A. Marsman, A.C. Vutha and E.A. Hessels, *A measurement of the atomic hydrogen Lamb shift and the proton charge radius*, *Science* **365** (2019) 1007.

[33] J. Brock, G. Gnanvo, P. Hemler, D. Kashy, N. Liyanage, G. Swift et al., 2021.

[34] G.G. Simon et al., *Absolute electron-proton cross sections at low momentum transfer measured with a high pressure gas target system*, *Nuclear Physics A* **333** (1980) 381.

[35] J.J. Murphy, Y.M. Shin and D.M. Skopik, *Proton form factor from 0.15 to 0.79 fm-2*, *Phys. Rev. C* **9** (1974) 2125.

[36] L.N. Hand, D. Miller and R. Wilson, *Electric and Magnetic Form Factors of the Nucleon*, *Rev. of Modern Phys.* **35** (1963) 335.

[37] A. Beyer et al., *The Rydberg constant and proton size from atomic hydrogen*, *Science* **358** (2017) 79.

[38] H. Fleurbaey et al., *New Measurement of the 1S−3S Transition Frequency of Hydrogen: Contribution to the Proton Charge Radius Puzzle*, *Phys. Rev. Lett.* **120** (2018) 183001.

[39] A. Grinin, A. Matveev, D.C. Yost, L. Maisenbacher, V. Wirthl, R. Pohl et al., *Two-photon frequency comb spectroscopy of atomic hydrogen*, *Science* **370** (2020) 1061.

[40] P.J. Mohr, D.B. Newell and B.N. Taylor, *CODATA Recommended Values of the Fundamental Physical Constants: 2014*, *Journal of Physical and Chemical Reference Data* **45** (2016) 043102.

[41] A. Antognini, F. Kottmann, F. Biraben, P. Indelicato, F. Nez and R. Pohl, *Theory of the 2S-2P Lamb shift and 2S hyperfine splitting in muonic hydrogen*, *Annals Phys.* **331** (2013) 127.

[42] I.T. Lorenz, H.-W. Hammer and U.-G. Meissner, *The size of the proton: Closing in on the radius puzzle*, *The European Physical Journal A* **48** (2012) 151.

[43] G. Lee, J.R. Arrington and R.J. Hill, *Extraction of the proton radius from electron-proton scattering data*, *Phys. Rev. D* **92** (2015) 013013 [`1505.01489`].

[44] K. Griffioen, C. Carlson and S. Maddox, *Consistency of electron scattering data with a small proton radius*, *Phys. Rev. C.* **93** (2016) 065207.

[45] M. Horbatsch and E.A. Hessels, *Evaluation of the strength of electron-proton scattering data for determining the proton charge radius*, *Phys. Rev. C* **93** (2016) 015204 [`1509.05644`].

[46] J.M. Alarcón, D.W. Higinbotham and C. Weiss, *Precise determination of the proton magnetic radius from electron scattering data*, *Phys. Rev. C* **102** (2020) 035203 [`2002.05167`].

[47] Z.-F. Cui, D. Binosi, C.D. Roberts and S.M. Schmidt, *Fresh extraction of the proton charge radius from electron scattering*, `2102.01180`.

[48] PRAD collaboration, *PRad-II: A New Upgraded High Precision Measurement of the Proton Charge Radius*, `2009.10510`.

[49] MUSE collaboration, *The MUon Scattering Experiment (MUSE) at the Paul Scherrer Institute*, *PoS* **NuFACT2018** (2018) 136.

[50] E1027 collaboration, *The MUSE experiment at PSI: Status and Plans*, *PoS* **NuFact2019** (2020) 076.

[51] B. Adams et al., *COMPASS++/AMBER: Proposal for Measurements at the M2 beam line of the CERN SPS Phase-1: 2022-2024*, .

[52] Bernauer, Jan C., *The proton radius puzzle - 9 years later*, *EPJ Web Conf.* **234** (2020) 01001.

[53] A1, MAGIX collaboration, *Operation and characterization of a windowless gas jet target in high-intensity electron beams*, *Nucl. Instrum. Meth. A* **1013** (2021) 165668 [`2104.13503`].

[54] A. Vorobyov and A. Denig, *MAMI A2 Proposal (PRES): High precision measurement of the ep elastic cross section at small Q2*, 2017.

[55] Suda, T., *Elastic electron scattering off protonusing 60 MeV electron linac of Tohoku University*, 2018.